

October 21, 1999

## Analysis and Theory of Multilayer Desorption: Ag on Re(0001)

S.H. Payne, G. Ledue, J.C. Michael, and H.J. Kreuzer

Department of Physics, Dalhousie University, Halifax, N.S. B3H 3J5, Canada

R. Wagner and K. Christmann, Institut fuer Physikalische and Theoretische

### Abstract

A multilayer lattice gas model including steps is set up to calculate the temperature programmed desorption spectra and other data for silver on two surfaces of Re. A careful comparison of isosteric and threshold analyses of the experimental data and the theoretical spectra is made. We discuss the effect of small temperature inhomogeneities on the spectra and on the desorption energies and prefactors obtained by an Arrhenius analysis. A rate subtraction procedure commonly used to analyze multilayer desorption data is shown to be unnecessary. Layer plots are presented and some general features for overlapping desorption peaks are discussed.



## I. Introduction

The study of the adsorption and multilayer growth of metals on metals by thermal desorption is still attracting considerable attention twenty-five years after the pioneering work of Bauer et al.<sup>1</sup> In recent papers a careful study was made of silver films grown on a rhenium(0001) surface.<sup>2</sup> The TPD (temperature programmed desorption) spectra are, in their qualitative features, somewhere in between those of Au and Cu on Mo(100) which have analyzed and modeled in a previous paper.<sup>3</sup> The common leading edge in the spectra implies zero order desorption from co-existing phases in both the first and second adlayers, however, the break from the leading edge is not as sharp and the drop on the high temperature side not as sudden as for example, for Cu on Mo(100). In addition, the fact that a silver atom is slightly larger than the lattice unit cell on the Re(0001) surface raises questions concerning lattice mismatch and incommensurability. It is argued in the experimental paper that this question can be answered by an analysis of the TPD data. When desorption peaks overlap, as occurs in this system for the peaks from the first and second (and of course all higher) adlayers, it is often suggested that a suitable subtraction should be done before an Arrhenius analysis of the data is attempted. We have seen in our previous analysis of the Cu/Mo(100) system that such a procedure is misleading and, indeed, unnecessary. We will demonstrate this again for the present system. Lastly, the TPD data for Ag on Re(0001) are such that the effect of small temperature inhomogeneities across the surface and/or nonlinearities in the heating rate can be identified when a detailed comparison between theory and experiment is performed.

A careful inspection of the TPD traces<sup>2</sup> for low initial coverages shows a shift of the desorption peaks to lower temperatures with increasing coverage up to about 0.2 ML, whereafter the peaks shift to higher temperatures. The initial shift to lower temperatures is unexpected for a system which must have predominantly attractive interactions for co-existing phases. Several reasons come to mind for this shift: (i) repulsive interactions will cause a shift to lower temperatures but their range must be beyond third neighbors with no attraction for nearer neighbors as this would cause clustering. On the other hand, because beyond 0.2 ML the system exhibits co-existence, the lateral interactions would need to change sign. This is unreasonable from an electronic point of view. (ii) Associative desorption would also shift the desorption peaks to lower temperature. But only Ag atoms have been detected.

(iii) A very small sticking coefficient at low coverages rising sharply at 0.2 ML would produce a shift but this is also in contraction to experiment which shows that the sticking coefficient is unity (at least at low temperature).  
 (iv) Another obvious mechanism is adsorption at more strongly bound defect sites, e.g. steps, followed by adsorption onto more weakly bound terrace sites. As we will see this can easily account for the observed shift.

At low temperatures (400K) STM images show that the rhenium surface has terraces of varying widths, as small as 10 unit cells and as wide as 1000 cells. These images also show that adsorption of silver begins at the step sites forming clusters onto the terraces. If these step densities were maintained up to the desorption temperature their effect on desorption would be restricted to initial coverages of less than 10% and 0.1%, respectively, and could not account for the downward shift up to 0.2 ML. Because we have no direct evidence, either from STM or from LEED, of the nature of the substrate surface in the desorption range, we treat the step density as a parameter in our theory and find the best (minimal) value that fits the TPD data.

## II. Lattice Gas Model

We briefly outline our theoretical approach. We model the adsorption of Ag on Re(0001) surface by a lattice gas with hexagonal symmetry. The steps are incorporated in our lattice gas model, as developed in previous papers on adsorption and desorption on stepped surfaces,<sup>6,5</sup> introducing three different adsorption sites, namely on the terraces (t), on the edges of the steps (e), and at the base of the steps (b), see Fig.1. Our only approximation at this stage is to assume that the terrace width is uniform as it would be in a well prepared stepped surface, rather than being variable as it no doubt is on the Re(0001) surface. We adjust the terrace width so that the fraction of energetically different (base) sites is about 0.15. In addition, the lattice gas model allows for multilayer growth as developed earlier.<sup>4</sup>

The energetics of the two-layer multi-site lattice gas model are given by a hamiltonian

$$\begin{aligned}
 H = & \sum_i [E_t^{(1)} t_i^{(1)} + E_b^{(1)} b_i^{(1)} + E_s^{(1)} e_i^{(1)}] \\
 & + \sum_i \sum_{\langle i, i' \rangle} [V_t^{(1-2)} t_i^{(1)} t_{i'}^{(2)} + V_b^{(1-2)} t_i^{(1)} b_{i'}^{(2)} + V_t^{(1-e)} t_i^{(1)} e_{i'}^{(2)} + V_b^{(1-e)} b_i^{(1)} e_{i'}^{(2)}]
 \end{aligned}$$

$$\oplus \sum_{\langle i, i' \rangle} [V_{1,2}^{(t-t)} t_i^{(1)} t_i^{(2)} + V_{1,2}^{(b-e)} e_i^{(1)} b_i^{(2)}] + \dots \quad (1)$$

Here  $i$  labels the adsorption sites and  $j=1,2$  the first and second layer. The occupation numbers  $t_i^{(j)}$ ,  $b_i^{(j)}$  and  $e_i^{(j)}$  are zero or one depending on whether the terrace, base or edge sites  $i$  in layer  $j$  are empty or occupied. The single particle energies are given, here for the terrace sites, by

$$E_t^{(j)} = -V_t^{(j)} - k_B T \ln(q_{3t}^{(j)}) \quad (2)$$

where  $V_t^{(j)}$  is the positive binding energy of a single particle to rhenium for  $j = 1$  and to a silver atom in the first layer for  $j = 2$ . Likewise,  $q_{3t}^{(j)}$  are the single particle partition functions accounting for the vibrations of a silver atom perpendicular and parallel to the surface; they are approximated by a product of three harmonic oscillators with frequencies (here for the terrace sites)  $\nu_{tx}^{(j)}$ ,  $\nu_{ty}^{(j)}$ , and  $\nu_{tz}^{(j)}$ , different in the first and second layer and for the different adsorption sites, generally. We restrict the intra- and interlayer lateral interactions to be to nearest and some next-nearest neighbors which is sufficient for systems with mainly attractive interactions.

To describe the adsorption and desorption kinetics we make use of the fact that in the temperature range of desorption surface diffusion is so fast on the time scale of desorption that during desorption quasi-equilibrium is maintained in the remaining adsorbate. That is to say, as particles desorb the remaining adsorbate redistributes itself so that the distribution among the various sites and layers and all correlation functions are those of equilibrium at the instantaneous temperature and the remaining coverage. Under such conditions (of quasi-equilibrium) the adsorbate is completely described by the partial coverages, e.g. for the  $N_t^{(j)}$  terrace sites in layer  $j=1,2$ ,

$$\theta_t^{(j)} = \frac{1}{N_t^{(j)}} \sum_i \langle t_i^{(j)} \rangle \quad (3)$$

These partial coverages are subject to kinetic equations

$$\frac{d\theta_t^{(j)}}{dt} = S_t^{(j)}(\theta, T) \frac{a_t \lambda_{th}}{h} P - S_t^{(j)}(\theta, T) \frac{a_t}{\lambda_{th} q_{3t}^{(j)}} \frac{k_B T}{h} e^{-V_t^{(j)}/k_B T} \frac{\theta_t^{(j)}}{1 - \theta^{(j)}} e^{\mu_a^{(int)}/k_B T} \quad (4)$$

and similar equations for the other partial coverages. Here  $a_t$  is the area of a terrace adsorption site,  $\lambda_{th} = h/\sqrt{2\pi mk_B T}$  is the thermal wavelength of a silver atom of mass  $m$ ,  $P$  is the pressure, and

$$\theta^{(j)} = \theta_t^{(j)} + \theta_e^{(j)} + \theta_b^{(j)} \quad (5)$$

is the coverage in the  $j$ -th layer.  $\mu_a^{(int)}$  is the part of the chemical potential of the adsorbate accounting for the energetic differences in the various sites and layers and also for all lateral interactions ( $\mu_a^{(int)} = 1$  for a homogeneous surface and in the absence of lateral interactions); its dependence on temperature and coverage will be calculated on the basis of the hamiltonian (1) employing the transfer matrix method, a standard procedure of statistical mechanics and our preferred choice.<sup>7</sup>

The sticking coefficients,  $S_t^{(j)}$ , etc. are a measure for the efficiency of energy transfer in adsorption, and thus are temperature and coverage dependent. Since energy supply from the substrate is required for desorption, the sticking coefficient, albeit usually at a higher temperature, must appear in the desorption rate by the detailed balance argument. The sticking coefficient cannot be obtained from thermodynamic arguments but must be calculated from a microscopic or mesoscopic theory or be postulated in a phenomenological approach, based on experimental evidence for a particular system or some simple arguments. For silver on Re(0001) we can safely assume that all sticking coefficients are constant and unity.

### III. Theoretical Results

To apply the above theory for the calculation of TPD spectra (for silver on Re(0001)) we proceed as follows: starting at the lowest initial coverages we note that the peaks of the TPD spectra<sup>2</sup> shift to lower temperatures for increasing initial coverages up to about 0.2 ML. As lateral repulsions of short range (between nearest or even next nearest neighbor sites) have little effect at such small coverages we assume that this shift is due to the initial occupation of defect sites, i.e. steps, followed by adsorption onto more weakly bound terrace sites. This coverage implies that the terrace width is about 6-8 rows of adsorptions sites. To obtain a good fit for coverages below 0.2 ML we adjust the parameters in the site free energies,  $E_t^{(1)}$ ,  $E_b^{(1)}$  and  $E_e^{(1)}$ , involving both binding energies and vibrational frequencies. In principle these could

be obtained from ab initio calculations or taken over from other, independent measurements such as vibrational spectroscopy or from the analysis of equilibrium data. Neither is available for the present system and we adjust these parameters to the peak positions and the widths of the lowest coverage TPD curves. From STM studies<sup>9</sup> we know that the base sites are more strongly bound and we find a binding difference to the terrace sites of about 48 kJ/mole; to keep the number of adjustable parameters to a minimum we assume  $E_t^{(1)} = E_e^{(1)}$  and equal vibrational frequencies for all sites. Next, because of the common leading edge in the TPD spectra, we expect that the lateral interactions are attractive and adjust their strengths to get a good fit up to monolayer coverage. Again for simplicity, we assume first neighbor interactions only (generally a good assumption for systems with attractive lateral interactions) and take them the same between all nearest neighbors on the terraces and for neighboring edge and base atoms across the steps. We find  $V_1^{(\alpha-\beta)} = -12\text{kJ/mole}$  ( $\alpha, \beta = t, e, b$ ). The overall result for the first monolayer is in good agreement with experiment, Fig.2. The fact that the leading edge in the theory is not as well-defined as in the experiment has no physical background but is simply due to the fact that in our implementation of the transfer matrix method we were restricted by computer memory to use a strip width equal to the terrace width.<sup>7</sup> We have checked the dependence of the fit on the width of the terraces; a 6-row terrace gives the best fit. This is at odds with the STM data, but one has to keep in mind that those images were taken at much lower temperatures. Also, nothing is known about the effect of Ag adsorption on the quality of the surface at high temperatures. (Klaus, Can you add something here, please).

Looking at the spectra for initial coverages between 1 and 2ML we repeat this procedure to get the parameters for the second layer, keeping the vibrational frequencies the same as in the first monolayer but adjusting binding energies and lateral interactions. For coverages just above a monolayer the peak positions are shifted to higher temperature relative to the leading edge of the second layer. Because this is not seen on a homogeneous surface we attribute this to the fact that the second layer also forms at the base sites first. This is due to the fact that a second layer atom at a base site is not only bound more strongly to the first layer than one of its second layer terrace neighbors but also (for equal lateral interactions between second layer atoms) interacts attractively with two nearest neighbor first layer edge atoms (in the completed monolayer) of an adjacent terrace. Again, to keep the number of

parameters at a minimum we impose identical binding energy differences between first and second layer sites,  $V_{\alpha}^{(1)} - V_{\alpha}^{(2)} = 62\text{kJ/mole}$ , and also the same type of intralayer interactions for the second layer as for the first,  $V_2^{(\alpha-\beta)} = -11\text{kJ/mole}$  ( $\alpha, \beta = t, e, b$ ). For the additional attraction between the second layer base and first layer edge atoms we get  $-17\text{kJ/mole}$  for the best fit.

In Fig.2 we show a **good** fit to the experimental data with the corresponding parameters listed in the figure caption. As a general feature the theoretical spectra are slightly higher at the peaks and consequently narrower than the experimental data. We will discuss this small discrepancy below. In obtaining the theoretical fit to the experimental data we renormalized the rates to obtain initial coverages that are lower by a factor 0.95 than those previously published. This was necessary in order that the monolayer desorption trace coincided with that obtained from the theory.

To understand the kinetics of this system we have extracted, from the theory, the partial desorption rates from the first and second layer and also from the various adsorption sites. As the partial rates from the first and second layer, Fig. 3(a), clearly indicate, desorption, and thus adsorption, is layer by layer. Looking first at desorption from a full monolayer we find that it starts at the temperatures at which the second layer itself desorbs. However, as the initial coverage is increased above a monolayer the partial desorption rate from the first layer,  $-d\theta^{(1)}/dt$ , is suppressed up to temperatures where the second monolayer has almost completely disappeared. And this onset of first layer desorption is to higher temperature with higher initial coverage. This fact has a very important consequence for the analysis of TPD spectra for initial coverages larger than 1ML, namely, it is inappropriate to subtract the TPD spectrum for initial coverage of 1 ML from the spectra with higher initial coverages to obtain the TPD spectra of the second layer alone: this does not work, and gives erroneous results for desorption energies and prefactors! Indeed, it is totally unnecessary for any Arrhenius analysis, as we will show below. This is, at first sight, surprising since the overlapping desorption peaks suggest that the energetics of adsorption in the first and second layers are quite similar so that, in a system maintained in quasiequilibrium by fast surface diffusion (and by implication fast particle exchange between layers) in the temperature range of desorption.

**Some site desorption rates**,  $-d\theta_t^{(j)}/dt$ , are shown in Fig.3 (b). Looking first at initial coverages below a monolayer, we see that the interior terrace

sites empty out first followed by those terrace and edge sites which are adjacent to the strongly bound base sites which remain occupied to the highest temperatures. A similar situation pertains for initial coverages larger than a monolayer.



The growth modes can be followed in detail in the (equilibrium) partial site coverage plots,  $\theta_t^{(j)}(\theta)$ , in Fig.3(c). Starting at the lowest coverages the base sites fill first up to a coverage of about 1/6 ML at which stage edge sites and also terrace sites start to be occupied because their attraction to the base sites compensates for their lower binding energies. This repeats when the second layer fills up, and for both layers more mixing of site occupations occurs at higher temperatures. Despite this nonuniform filling of the three types of sites, the partial coverages in the first and second layers rise linearly with coverage such that  $\theta^{(1)} = \theta$  for  $\theta < 1$  and  $\theta^{(2)} = (\theta - 1)$  for  $\theta > 1$ .


## IV. Analysis of Spectra


Having obtained good agreement of the theoretical TPD spectra with the experimental data, we can infer additional information about the system from a proper Arrhenius analysis of both sets of spectra. The purpose of an Arrhenius analysis is to reduce the multitude of TPD traces for different initial coverage to just two coverage dependent functions, namely the desorption energy and the effective prefactor, obtained by parametrizing the desorption rate as

$$\frac{d\theta}{dt} = -\nu_{eff}(\theta)e^{-E_d(\theta)/k_B T} \quad (6)$$




Such an analysis,<sup>13</sup> for TPD data obtained by variation of initial coverages, can be performed using the isosteric or threshold method. For 'perfect' data (i.e without systematic or statistical errors, such as calculated spectra) these two analyses (and heating rate variation) give identical results. For the theoretical spectra in Fig.2 the resulting desorption energy and prefactor are shown in Fig.4. At zero coverage the desorption energy is, to within vibrational contributions, the binding energy of the base sites. With increasing coverage  $E_d(\theta)$  reflects firstly the effective lowering of the binding energy in the first layer as the weaker bound edge and terrace sites become occupied. This trend is reversed above 1/6 ML as a result of the lateral attraction. At the completion of a monolayer,  $E_d(\theta)$  drops suddenly by an amount roughly



equal to the binding difference for first and second layers. Because for a system in quasi-equilibrium the desorption energy (plus  $k_B T/2$ ) is the isosteric heat of adsorption (in the absence of precursors) we expect the desorption energy from the second layer to be greater than the cohesive energy of the bulk metal (274kJ/mole **of** silver). 

The lateral attractions, deduced from fitting the leading edges of the experimental spectra,<sup>3</sup> are such that for a homogeneous substrate the temperature range of desorption is below the critical temperature for the coexistence of dilute and condensed phases,  $T_c \simeq V^{t-t}$  for a hexagonal lattice. This would lead to (i) sharp leading edges in the TPD spectra, and (ii) to a corresponding coverage-independent desorption energy **plateau** over the coexistence region (away from zero and full monolayers) after an initial rise in the low coverage (dilute) regime from the single particle binding energy,  $V_t$ , to  $V_t + 3V^{t-t}$ . This is shown in Fig.4 as a dash-dotted line. That we see a rise around 1/2 and 3/2 ML for the full model with steps is largely due to our computational limitation discussed earlier. The prefactor in Fig.4(b) shows a coverage dependence mimicking that of the desorption energy. 

We have also re-analyzed the experimental data performing both an isosteric<sup>10,11</sup> and a threshold<sup>12</sup> Arrhenius analysis using the ASTEK software package.<sup>13</sup> The results for the threshold analysis have been included in Fig.4 including our estimate of error resulting from the choice of fractional depletion used in the analysis. We should also point out that the threshold analysis is sensitive to the background subtraction which could not be assessed. Overall magnitudes of desorption energy and prefactor are in good agreement with the theoretical values and qualitative features such as the rise below about 0.2 ML and the drop at 1 ML are in common.

The results of this threshold analysis of the experimental TPD spectra are in some disagreement with those obtained in the **previously**<sup>9</sup> using the isosteric analysis (we repeat again that for 'perfect' data these two procedures should **produce** the same result). We have therefore repeated the isosteric analysis using again the ASTEK **programme**, Fig.5. Similar values of desorption energy and prefactor are found in the mid-coverage range of the first monolayer, **and a decrease below 0.3 ML (where it should rise to reflect the binding to the stronger base sites)**. The difference in the desorption energy between the mid-coverage regime of the first and second layer, respectively, is only half of what the threshold analysis gives, and what we need in the theory to fit the peak separation.   
  


Next we illustrate the inadmissability of subtracting the monolayer desorption trace from the higher initial coverage spectra. As we discussed above for overlapping first and second layers there is a delay in the onset of desorption from the first layer to higher temperatures for initial coverages larger than a monolayer. This implies, among other things, that the remaining first layer peak gets modified. We can see this very clearly in the theoretical spectra when we subtract the  $\theta_0=1$  desorption trace from those with larger  $\theta_0$ , see Fig.6 (a), where this modification leads to a residual peak at the position of the submonolayer spectra. For comparison we also show the actual second layer partial rates for two initial coverages (cf. Fig. 3(a)). The subtracted rates are less throughout the range of the second layer desorption because of the erroneous subtraction of the  $\theta_0$  rate which starts well below the second layer peak. The difference appears in the residual peak at higher temperatures.

A threshold analysis of these (subtracted) spectra yields results close to those of the unsubtracted spectra for all  $\theta_0$ , because the initial rates (at the lowest temperatures) are least effected by the subtraction. However, an isosteric analysis produces different results in the low coverage regime of the second layer due to the existence of the residual peak around 1,000K. This is shown in Fig. 5 as a drop below about 1.4 ML. For completeness we also show the results of an isosteric analysis of the subtracted experimental second layer spectra (Fig.6 (b)) in Fig.5 (circles). The results differ of course from those of the analysis of the unsubtracted experimental spectra and also from the model data. There are a number of reasons for this such as our different normalization of the initial coverages, and possibly the overall subtraction of a background from all desorption traces.

We will now show that the qualitative difference at low (submonolayer) coverage in the desorption energy and prefactor between the results from the threshold and isosteric analyses of the experimental data may be due to deviations in the temperature ramp from a perfectly linear and constant heating rate and/or inhomogenieties in the temperature across the sample surface. Whether this is the case for the present data is not clear without further experiments. However, it is worth pointing this effect out because it stipulates high quality temperature control in TPD experiments. To show this we have averaged the theoretical spectra over a small temperature range of 10 K, i.e. assuming an inaccuracy in the temperature measurements or in the homogeneity of the temperature across the sample of about 1%. The effect

on the spectra themselves is that the peaks get broadened and lowered with the trailing edge less precipitous, the more so the sharper the peaks. The latter fact has the immediate consequence in the isosteric Arrhenius analysis to lead to lower desorption energies and prefactors at low coverages, solid line in Fig.7. Most importantly, the isosteric Arrhenius analysis of these smeared (theoretical) data show the same low coverage behaviour of the desorption energy and prefactor as the isosteric analysis of the experimental data. Averaging over a larger temperature window will enhance the drop even further. Temperature inhomogeneities can be viewed as a non-equilibrium effect and as such will result in isosteric rates which are patently not linear in  $1/T$ . This can be illustrated by plotting the differential desorption energy, i.e. the local slope of the Arrhenius plots. They vary for different initial coverages as shown in Fig.7, the solid line is simply the straight line approximation to the (curved) isosteres. The latter is qualitatively similar to the experimental data. The discontinuities in Fig.7 are not due to an error in the analysis but occur as the chosen isosteres cross the initial coverages of the TPD spectra. In this case two adjacent coverages sample the desorption rates at considerably different temperatures. Such effects are rarely seen in experimental data where they are averaged out by the noise in the rates. In any case, temperature inhomogeneities are a likely explanation why so many (isosteric) analyses of experimental data show a precipitous drop in both desorption energy and prefactor for low coverages where in addition all experimental uncertainties have accumulated.

Additional evidence of temperature inhomogeneity is apparent in the TPD spectra for initial coverages greater than 2 ML, which should show a well-defined common leading edge (as it does for 2 ML) expected for multilayer nobles, in particular close to their melting temperature where surface diffusion will maintain adsorbate equilibrium during desorption.

There is a straightforward check to lend further credence to our hypothesis and that is to perform a threshold analysis on the TPD data. In this case we only take the data over a small depletion of the initial coverage, and the effect of temperature inhomogeneities can be reduced substantially. Indeed, performing a threshold analysis on the temperature smeared theoretical spectra we recover completely the results of the analysis of the unsmeared data including the rise of the desorption energy (reflecting the larger binding at the steps) and prefactor towards zero coverage.

The last point we want to make is concerning the layer plots. Both the

theoretical and the experimental spectra, Fig. 8, show a shift of the minima at about monolayer initial coverage to lower coverages. The abrupt change in the respective shifts of the minima positions near the completed monolayer has been interpreted as the signature of the fact that silver atoms are too large to fit into the Re(0001) lattice structure. Thus for coverages larger than 1 ML the silver lattice should expand leading to a reduction in the maximum coverage possible. We want to point out in addition that the shifts in the minima of the layer plots themselves have nothing to do with lattice mismatch. In our theory there is no such mismatch, yet the theoretical spectra exhibit the same trend in moving the minimum to smaller coverages, as observed in the experimental layer plots. This results simply from the fact that the first and second layer peaks overlap. Indeed, if we artificially reduce the gap between the two peaks (by raising the binding energy of Ag in the second layer) we can increase the shift in the interlayer minimum by up to 10 percent. This shift also has nothing to do with the fact that there are attractive interactions between adsorbed silver atoms. Reducing the lateral interactions to zero, or even making them repulsive (which changes the shape of the two desorption peaks considerably removing the leading edge altogether) does not effect the qualitative picture of the shift of the minimum. On the other hand the shift is absent when the second layer peak is completely separated from that of the first layer.

## V. Desorption from a surface with high step density

We recall that in our attempt to model an important detail in the low initial coverage TPD spectra, namely the shift of the desorption peaks to lower temperatures, we invoked a step density (of 6 - 8 adsorption sites per terrace) which is higher than low temperature STM data suggest. To shed further light on this problem we have performed TPD experiments from a surface with a high step density with terrace widths of about 3 adsorption sites. If our theory is correct we should, without changing any parameters except the terrace width, expect a fit to these data. Indeed, this is the case, see Fig.9a and b. One qualitative difference between the submonolayer spectra of Fig. 9 and Fig.2 is the disappearance of the common leading edge. This is simply the consequence of the size effect<sup>6,5</sup> associated with small systems in which phase transitions are suppressed.

---

The major deviation is the width and peak position in the submonolayer

regime. The minimal changes needed to get a better fit, Fig.9c, is an increase in the binding energies to the surface and a decrease in the lateral attraction, both by about 10%, keeping the difference in binding energies between step and terrace sites the same. This is easily understood when one considers that this surface with a high step density is closer to an open surface such as Re(...) if the steps were arranged in a regular pattern. Such open surfaces typically have a larger electronic density in the surface region which can be used by the adatoms for stronger binding to the surface, thus reducing concomitantly the availability of electrons for lateral binding.

We have performed an Arrhenius analysis of Fig. 9c; the results for desorption energy and prefactor are included in Fig. 4 (dashed lines). There is an overall upward shift in the desorption energy. For submonolayer coverages the energy drops smoothly till about 0.3 ML at which time the base sites are fully occupied, and remains constant until completion of the first monolayer, again a signature of the reduced overall attraction. The drop at a monolayer is again indicative of essentially layer-by-layer growth but is not as pronounced as for the wider terraces. Prefactors for the two surfaces are essentially the same because we kept the same surface vibrational frequencies.

Although the data of Fig.9a are not of the high quality of those in Fig.2 we nevertheless performed isosteric and threshold analyses, and obtained desorption energies and prefactors that were systematically lower by up to 60 kJ/mol and two orders of magnitude, respectively, as compared to both the values for the smooth surface and also as compared to the theoretical model of Fig.9c. This is obviously not an acceptable result, and emphasizes the fact that unless the TPD spectra are of sufficient quality, one should not trust the analysis but attempt a direct theoretical modeling of the spectra and analyse these instead. Further analysis of this system in combination with an analysis of the adsorption and desorption of Cu from the same surface will be given elsewhere.

## VI. Summary

In this paper we have set up a lattice gas model for the adsorption of silver on Re(0001) up to two monolayers. Careful inspection and analysis of experimental TPD data resulted in the following details of the model:

- (1) The leading edge of the TPD spectra in both the first and second

layers indicate attractive lateral interactions strong enough to maintain the adsorbate below its critical temperature throughout the desorption range.

(2) The substantial shift of the TPD peaks to lower temperatures for initial coverages below about 0.2 suggest the presence of more strongly bound adsorption sites. These have been incorporated in the lattice gas model as step sites in addition to (the more weakly bound) terrace sites.

(3) Because the silver atoms can be assumed to be highly mobile throughout the desorption range we can assume that quasi-equilibrium is maintained so that the kinetics can be formulated within the framework of nonequilibrium thermodynamics.

(4) To evaluate the chemical potential of the stepped multilayer lattice gas, needed for thermodynamic and kinetic properties, we have employed transfer matrix methods.

Fitting the model to the experimental TPD data allowed us to extract the parameters of the lattice gas such as the single particle binding energies at terrace and step sites in the first and second layers, vibrational frequencies of silver atoms with respect to the surface, and lateral attractive interactions. To keep the set of parameters to a minimum we assumed that the frequencies are the same for all sites and both layers, and that lateral interactions are between nearest neighbors only and equal between all sites within each layer.

Although the model produced a satisfactory fit to the TPD data, we explored possible origins of small but systematic deviations. To do this we re-analyzed the experimental data performing Arrhenius analyses to extract desorption energies and prefactors which we then compared to those obtained from the theoretical spectra. We employed both the threshold and the isosteric methods which of course give identical results for 'perfect' data such as the theoretical spectra. However, for 'real' data which always have error bars associated with them, even for 'good' data, as the ones analyzed here, the threshold analysis is more accurate. The reason is that any inhomogeneities in temperature, either due to small instabilities in the heating rate or due to uneven heating of the substrate, have a cumulative effect on TPD spectra so that the high temperature/low coverage part is the most affected. This, we show, results in a substantial drop in both desorption energy and prefactor towards zero coverage when the isosteric method is used whereas a threshold analysis produces a rise reflecting the stronger binding at the edge sites.

To simulate these temperature inhomogeneities we have smeared the theoretical TPD data over a range of 10 K, or 1% of the desorption temperature

and recover the trends exhibited by the analyses of the experimental data. This, once more, suggests that it is mandatory to do both threshold and isosteric analyses to extract the maximum amount of information out of TPD data: Although the threshold analysis gives a more accurate picture of the energetics of the adsorbate, the isosteric analysis gives information, among others, on possible temperature inhomogeneities. One should also bear in mind that any non-equilibrium effects such as temperature inhomogeneities will result in curved isosteres in the Arrhenius plots which advantageously are analyzed using the differential desorption energies along the isostere instead of a linear approximation.

Our last point concerns the standard practice in the analysis of multiplexed desorption peaks to extract single peak spectra by some subtraction procedure. In this system, this practice amounts to subtracting the monolayer desorption trace from those of higher initial coverages. As we show in detail this procedure is unwarranted because the first layer desorption trace (the partial desorption rate from the first layer) changes dramatically for initial coverages larger than one monolayer when the desorption peaks overlap. Not only that, the procedure is unnecessary because the analysis of the complete set of spectra can be done without impunity, in particular employing the threshold method.



What we hope to have shown in this paper is that the combination of theoretical modeling of the experiment together with a complete analysis of both experimental and theoretical 'data' yields the maximum information about a system and puts any interpretation on firmer grounds.

### Acknowledgement

The work at Dalhousie University was funded in part by grants from NSERC and the Office of Naval Research.



## References

- <sup>1</sup>E. Bauer, H. Poppa, G. Todd, and F. Bonczek, *J. Appl. Phys.* 45 (1974) 5164.
- <sup>2</sup>D. Schlatterbeck, M. Parschau, and K. Christmann. *Surf. Sci.* 418 (1998) 240.
- <sup>3</sup>S.H. Payne, H.J. Kreuzer, A. Pavlovska, and E. Bauer. *Surf. Sci.* 345:L1-L10, 1996.
- <sup>4</sup>S.H. Payne and H.J. Kreuzer. *Surf. Sci.* 338:261-278, 1995.
- <sup>5</sup>W. Widdra, P. Trischberger, W. Friess, D. Menzel, S.H. Payne, and H.J. Kreuzer. *Phys. Rev. B* 57:4111-4126, 1998.
- <sup>6</sup>S.H. Payne and H.J. Kreuzer. *Surf. Sci.* 399:135-159, 1998.
- <sup>7</sup>H.J. Kreuzer and S.H. Payne. *Theoretical Approaches to the Kinetics of Adsorption, Desorption and Reactions at Surfaces*. In *Computational Methods in Colloid and Interface Science*, ed. M. Borowko. (Marcel Dekker Inc., New York, 1999).
- <sup>8</sup>Transfer matrix calculations can be done routinely, for instance, with the ASTEK program package for the Analysis and Simulation of Thermal Equilibrium and Kinetics of gases adsorbed on solid surfaces, written by H.J. Kreuzer and S.H. Payne (available from Helix Science Applications, 618 Ketch Harbour Road, Portuguese Cove, N.S. B3V 1K1 Canada).
- <sup>9</sup>M. Parschau, D. Schlatterbeck, and K. Christmann. *Surf. Sci.* 376 (1997) 133.
- <sup>10</sup>D.A. King, T.E. Madey, and J.T. Yates, Jr., *J. Chem. Phys.* 55 (1971) 3236.
- <sup>11</sup>E. Bauer, F. Bonczek, H. Poppa, and G. Todd. *Surf. Sci.* 53 (1975) 5164.
- <sup>12</sup>E. Habenschaden and J. Küppers, *Surf. Sci.* 138 (1984) L147.
- <sup>13</sup>The Arrhenius analysis both for the experimental and the theoretical TPD spectra has been done with the ASTEK programme, see previous reference.





## Figure Captions

Fig.1: Sketch of the lattice gas model with adsorption sites

Fig. 2: TPD spectra for Ag/Re(0001) with a heating rate of 2.5 K/s. Dashed lines experimental data for initial coverages  $\theta_0 = 0.052, 0.11, 0.18, 0.25, 0.32, 0.40, 0.48, 0.55, 0.64, 0.73, 0.82, 0.93, 1.00, 1.14, 1.22, 1.27, 1.41, 1.55, 1.70, 1.77, 1.89, 1.95$ . Solid curves theoretical model with parameters:  $V_t^{(1)} = V_e^{(1)} = 227$  kJ/mol,  $V_t^{(2)} = 316$  kJ/mol,  $V_t^{(2)} = V_e^{(2)} = 164$  kJ/mol,  $V_b^{(2)} = 212$  kJ/mol,  $\nu_j^{(j)} = 6.0 \times 10^{12} \text{ s}^{-1}$  for  $j=1,2$  and  $i=t, b, e$ ;  $V_1^{(\alpha-\beta)} = -12.2$  kJ/mol,  $V_2^{(\alpha-\beta)} = -10.8$  kJ/mol,  $V_{1-2}^{(\epsilon-\beta)} = -17.5$  kJ/mol.

Fig.3: (a) Model partial desorption rates from the first (solid lines) and second (dashed lines) layers for initial coverages  $\theta_0 = 0.11, 0.55, 1.0, 1.46, 1.95$ . (b) Individual site contributions,  $-d\theta_i^{(j)}/dt$  to these rates: base sites - dotted lines, terrace sites - solid lines, edge sites - dashed lines. (c) Equilibrium layer partial coverages,  $\theta_i^{(j)}(\theta)$ , (long-dashed lines) for temperatures spanning the desorption range  $T = 700, 1000$  K; and corresponding site occupations  $\langle \alpha_i^{(j)} \rangle$  for  $\alpha = t, b, e$  with line types as above.  $T=700$  K curves exhibit the sharpest features.

Fig. 4: (a) Desorption energy, from an Arrhenius analysis of experimental and theoretical TPD spectra: solid lines - analysis of theoretical curves in Fig.2; dashed lines - analysis of model spectra for a homogeneous Re substrate with same intralayer interactions as spectra of Fig.2; crosses - from a threshold analysis of experimental spectra of Fig.2.

(b) Corresponding prefactors from eq.(6),  $\nu_{eff}(\theta)/\theta$ .

Fig. 5: Desorption energies (a) and prefactors (b) from an isosteric analysis of the experimental data. Crosses: analysis of the complete set of spectra up to 2 ML, dashed lines in Fig.2. Circles: analysis of the second layer after (erroneous) subtraction of the 1 ML rate curve, see Fig.6 (b). Solid line: corresponding results for such a subtraction of the model spectra, see Fig.6 (a).

Fig. 6: TPD rates obtained by subtracting the monolayer rate from all higher initial coverage curves in Fig.2, for model (a) and experimental spectra (b). Dashed lines in (a) are partial desorption rates from the second layer for  $\theta_0 = 1.41$  and  $1.95$ .

Fig. 7: Desorption energies (a) and prefactors (b) from an isosteric analysis of model rates, averaged over a range of 10K to account for temperature inhomogeneities, for  $\theta_0 = 0.1 \dots 1.0$  in steps of 0.1. Solid line is a linear fit

to the (curved) isosteric rates (as a function of  $1/T$ ). Crosses: local slopes of these isosteres.

Fig. 8: Layer plots of the desorption rates of Fig.2.

Fig.9: TPD spectra for Ag from a stepped Re surface with a heating rate of 4.1 K/s. (a) Experimental data for initial coverages  $\theta_i = 0.02, 0.1, 0.18, 0.26, 0.37, 0.44, 0.56, 0.66, 0.74, 0.80, 0.88, 0.97, 1.10, 1.18, 1.35, 1.45, 1.56, 1.59, 1.88, 2.0$ . (b) Theoretical model with parameters of Fig.2, except for terrace width of 3 sites instead of 6. (c) Theoretical model with binding energies and lateral interactions changed by 10 %:  $V_i^{(1)} = V_s^{(1)} = 227$  kJ/mol,  $V_b^{(1)} = 316$  kJ/mol,  $V_i^{(2)} = V_s^{(2)} = 164$  kJ/mol,  $V_b^{(2)} = 212$  kJ/mol,  $\nu_i^{(j)} = 6.0 \times 10^{12} \text{ s}^{-1}$  for  $j=1,2$  and  $i=t, b, e$ ;  $V_i^{(\alpha-\beta)} = -10.8$  kJ/mol,  $V_j^{(\alpha-\beta)} = -9.1$  kJ/mol,  $V_{1-2}^{(\alpha-\beta)} = -17.5$  kJ/mol for  $\alpha, \beta=t, b, e$ .

